PCCP

PAPER

View Article Online
View Journal | View Issue

Cite this: *Phys. Chem. Chem. Phys.*, 2018, **20**, 20070

Analysis of epoxy functionalized layers synthesized by plasma polymerization of allyl glycidyl ether

Anton Manakhov,*[a] Šárka Fuková,[bc] David Nečas,[b] Miroslav Michlíček,[bc] Sergey Ershov,[d] Marek Eliáš,[bc] Maxim Visotin,[ef] Zakhar Popov[a] and Lenka Zajíčková[bc]

Received 6th March 2018,
Accepted 8th July 2018

DOI: 10.1039/c8cp01452c

rsc.li/pccp

The deposition of epoxide groups by plasma polymerization opens new horizons for robust and quick immobilization of biomolecules on any type of substrate. However, as of now there are just very few papers dealing with the deposition of epoxy layers by plasma polymerization, probably due to the high reactivity of this group leading to a low functionalization efficiency. In this work we carried out an extensive experimental and theoretical investigation of plasma synthesis of epoxide groups from a low pressure allyl glycidyl ether (AGE) plasma. The influence of composite parameter W/F and the working pressure on the density of epoxide groups and the layer stability was thoroughly addressed. It was found that by increasing the working pressure it is possible to sufficiently raise the concentration of epoxide groups. The composite parameter W/F was shown to be a crucial parameter in affecting the density of epoxides. An optimal value of W/F of around 2.3 eV per molecule leading to the highest density of epoxides produced in the process at 15 Pa was revealed through FT-IR and XPS findings. This value correlates well with the *ab initio* calculations suggesting that the lowest bond dissociation energy belongs to the C–O bond of the epoxide ring. Therefore, in order to increase the density of epoxides deposited by plasma polymerization, a precursor molecule containing at least two epoxide rings is strongly advised to be employed.

1 Introduction

Epoxy-functionalized surfaces are attractive platforms for immobilization of bio-molecules thanks to their high reactivity towards amine and amide groups.[1–3] The conjugation of epoxy groups with primary, secondary and even tertiary amines can be realized at room temperature and without any catalyst.[4–6] The epoxy-groups are deposited onto a surface mainly by the silanization process,[7] though the production of homogenous layers by this substrate-dependent wet chemical method is challenging and requires tuning of many parameters.[8] Commercially available epoxy-functionalized glass slides are therefore of relatively high cost (>3 Eur cm^{-2}). The deposition of epoxy functionalized layers by an environment-friendly, relatively inexpensive and substrate-independent plasma polymerization technique exhibits, therefore, great potential for emerging technologies. There are, however, just very few papers dealing with the deposition of epoxy layers by plasma polymerization, probably due to the high reactivity of this group leading to a low functionalization efficiency.

The first promising results were obtained by plasma polymerization of glycidyl methacrylate (GMA) at low[9] and atmospheric pressure.[10] According to IR spectroscopy, the retention of epoxy groups increased with the GMA flowrate and the plasma OFF-time. Subsequent MALDI-ToF and XPS analyses of plasma polymerized GMA layers confirmed that a decrease of the plasma ON-time as well as an increase of the plasma OFF-time sufficiently reduced GMA fragmentation.[11,12] Unfortunately, the authors did not report the stability of GMA plasma polymers in water or other liquid environments. Moreover, recently it was found that GMA is a highly toxic and carcinogenic compound.

Another precursor that was used for the deposition of epoxy functionalized plasma polymers is allyl glycydyl ether (AGE).

[a] *National University of Science and Technology "MISiS", Leninsky pr. 4, Moscow 119049, Russia. E-mail: ant-manahov@ya.ru*
[b] *RG Plasma Technologies, CEITEC – Central European Institute of Technology, Masaryk University, Purkyňova 123, Brno 61200, Czech Republic*
[c] *Department of Physical Electronics, Faculty of Science, Masaryk University, Kotlářská 2, Brno 61137, Czech Republic*
[d] *Materials Research and Technology Department, Luxembourg Institute of Science and Technology, 5 avenue des Hauts-Fourneaux, Esch-sur-Alzette, Luxembourg*
[e] *Siberian Federal University, 79 Svobodny av., Krasnoyarsk, 660041, Russian Federation*
[f] *Federal Research Center KSC SB RAS, 50/38 Akademgorodok, Krasnoyarsk, 660036, Russian Federation*

Low pressure plasma polymerization of non-toxic AGE was studied in the research group of Griesser.[13,14] It was found that the density of epoxy groups in plasma polymerized AGE layers can be increased by reducing the duty cycle and plasma power, similarly to what was shown for GMA. Furthermore, modified AGE plasma polymers exhibited good anti-fouling properties, *i.e.* non-specific binding events can be prevented on these layers after quenching with ethanolamine.[13] However, the reported high thickness loss (40% after 24 h in methanol) of AGE plasma polymers would be a problem for bio-application of these layers. Hence, it is very important to pursue the optimization of AGE plasma polymerization through fine tuning of all deposition parameters, namely the AGE flowrate, the pressure, the power and the duty cycle.

In this work low pressure plasma polymerization of AGE is studied. The density of epoxy groups sufficient for the subsequent grafting of biomolecules accompanied by a good layer stability in water was targeted. The stability and chemical structure of AGE plasma polymers were investigated as a function of pressure and composite parameter W/F. It was found that a pressure increase has a positive effect on the retention of epoxide groups, but at the same time the layers deposited at high pressure exhibited low homogeneity and insufficient stability. The influence of the W/F parameter was shown to be rather complex and it is extensively discussed in the paper.

2 Materials and methods

2.1 Plasma setup

AGE plasma polymers were prepared in a standard Gas Energy Conference (GEC) stainless steel parallel plate reactor (Fig. 1a). The bottom electrode was capacitively coupled to a radio frequency generator working at a frequency of 13.56 MHz. AGE (98%, Sigma Aldrich) vapours were fed into the chamber through a grounded upper showerhead electrode, and the AGE flowrate was set by a needle valve. The distance between the electrodes was 50 mm. The bottom electrode with Si substrates (111, N-type, phosphorus doped, resistivity 0.5 Ω cm, double side polished, ON-semiconductor) was negatively DC self-biased due to an asymmetric coupling. The reactor was pumped down to 10^{-4} Pa by a combination of a membrane pump and a turbomolecular pump. The leak rate including wall desorption was below 0.02 sccm for all the experiments.

AGE was polymerized in pulsed wave plasmas at pressures of 10, 15 and 30 Pa. The pulse repetition frequency (PRF) was set to 2105 Hz to provide very short pulses. The duty cycle was varied between 10 and 3%, whereas the plasma power was altered in the range from 4 (the minimal possible value) to 25 W. A summary of the studied plasma deposition conditions as well as the thicknesses and compositions of the deposited layers is given in Table 1. The composite parameter W/F was calculated by using the formula described in ref. 15. The deposition time was adjusted to obtain the film thickness suitable for the FT-IR analysis with the exception of the layer deposited at W/F = 0.91 eV per molecule (due to the extremely low deposition rate, the layer thickness remained remarkably small even after 30 minutes of deposition).

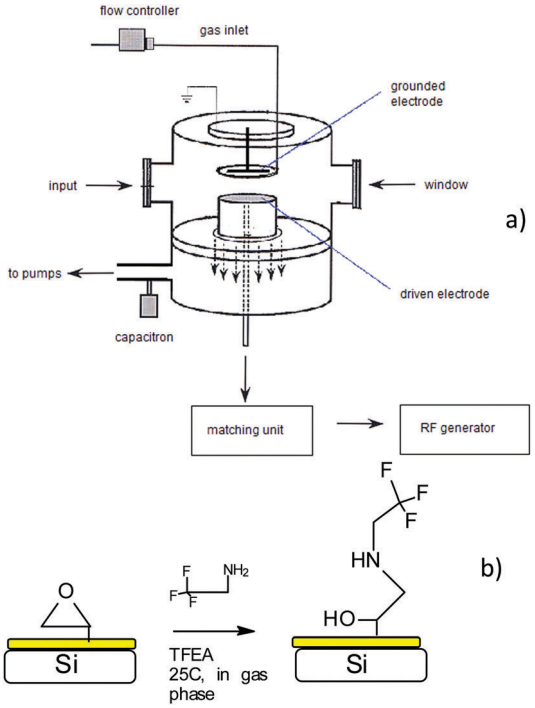

Fig. 1 Scheme of the plasma setup (a) and chemical derivatization of AGE plasma polymers (b).

Table 1 Summary of plasma conditions, layer thicknesses and elemental compositions

W/F (eV per molecule)	Power (W)	D.C. (%)	T_{on} (μs)	T_{off} (μs)	AGE flowrate (sccm)	Layer thickness (nm)	[C] (at%)	[O] (at%)
0.91	4	3	14	461	2	15	75.0	25.0
1.40	6	3	14	461	2	61	79.2	20.8
1.90	5	5	24	451	2	147	78.0	22.0
1.96	10	5.2	25	450	4	121	77.6	22.4
2.30	10	3	14	461	2	47	79.0	21.0
2.30	6	5	24	451	2	48	79.3	20.7
3.80	10	5	24	451	2	175	78.3	21.7
3.90	10	5.2	25	450	2	109	78.1	21.9
4.91	25	5.2	25	450	4	211	78.8	21.2
9.4	25	5	24	451	2	355	79.2	20.8
9.8	25	5.2	25	450	2	218	78.0	22.0
18.9	25	10	24	451	2	703	80.0	20.0

2.2 Optical characterization

The films on Si wafers were characterized by ellipsometry using a phase modulated Jobin Yvon UVISEL ellipsometer in the spectral region 1.5–6.5 eV with an angle of incidence of 65°. The data were fitted using a PJDOS dispersion model for polymer SiO_2-like materials[16] and a structural model of wedge-shaped non-uniform thin films.[17] The thickness and thickness non-uniformity were fitted as described elsewhere.[16,17]

2.3 XPS

The chemical composition of the surfaces was characterized by X-ray photoelectron spectroscopy (XPS) using an Axis Supra

(Kratos Analytical, England) spectrometer. The maximum lateral dimension of the analyzed area was 0.7 mm. To avoid differential charging of samples, spectra were acquired with charge neutralization. The spectra were subsequently normalized by shifting the hydrocarbon component CH_x to 285.0 eV. The spectra were acquired at a pass energy of 20 eV. The fitting of XPS data was done in the CasaXPS software (version 2.3.17) after the subtraction of the Shirley-type background employing Gaussian–Lorentzian (G–L) peaks with the fixed G–L percentage 30%. The values of binding energies (BEs) for carbon, nitrogen and oxygen environments were taken from the literature.[9,12,18,19]

2.4 AFM

The topography of film surfaces was measured using a Bruker Dimension Icon atomic force microscope (AFM) in tapping mode using standard probes. Large-area scans from 10 × 10 to 90 × 90 μm^2 were used for the investigation of particles incorporated in the films, film buckling and other large-scale topographical details, whereas the characterization of fine roughness was performed with small-area scans of 1 × 1 μm^2. Processing and statistical characterization of AFM data were carried out using Gwyddion software.

2.5 Chemical derivatization of epoxy groups

Gas phase chemical derivatization was performed on freshly prepared samples by their exposure to 2,2,2-trifluoroethylamine TFEA (98%, Sigma Aldrich) vapour. The reaction time was set to be 1 hour, and immediately after the reaction the samples were placed into a freezer and kept at −20 °C prior to XPS analysis. The schematic reaction is presented in Fig. 1b.

2.6 Computational methods

The molecule geometry and bond breaking energies were calculated with the help of the Density Functional Theory method (DFT) with the B3LYP exchange–correlation functional[20,21] and using the 6-311++G(d,p) basis set as implemented in the GAMESS code.[22] The methods were chosen as they are known to give good descriptions of AGE and similar compounds, *e.g.* ref. 23 and 24. The geometry was first optimized for singlet and triplet states. Then, it was found that the lowest energy state is a singlet and thus for this state the fragmentation *via* different bond fractures was estimated with each fragment being calculated separately. In the case of the epoxy group, breaking of a C–O bond was modeled by applying constraints on the opposite angles (between the other C–O bond and the C–C bond) as in the case of ordinary sp^3-hybrydized bonds. The energy of the double C=C bond conversion into a single C–C bond was estimated through the energy of the triplet–singlet transition, in which a bonding pi-bond is substituted by an anti-bonding pi*-bond.

3 Results

3.1 Optimization of the pressure

3.1.1 The AGE plasma polymer homogeneity and morphology.

The ignition of the discharge in pure AGE was possible at a power $P \geq 4$ W and a pressure $10 \leq p \leq 30$ Pa. The values of a negative D.C. self-bias for the AGE flowrate of 2 sccm are plotted as a function of power in Fig. 2.

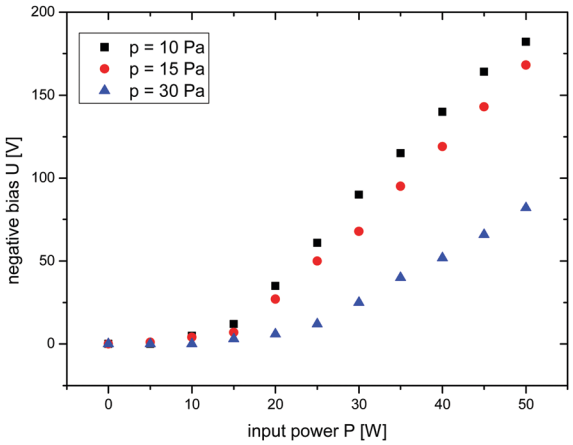

Fig. 2 The D.C. self-bias as a function of power and pressure for the discharge at an AGE flowrate of 2 sccm.

In order to optimize the pressure, it was decided to fix the power and the duty cycle at 25 W and 5.2%, respectively. This condition led to W/F of 9.8 eV. At 10 and 15 Pa, the AGE plasma polymerization resulted in the deposition of smooth and homogenous layers over the entire RF electrode surface, whereas the polymerization at 30 Pa led to the deposition of layers exhibiting many particles as AFM measurements revealed (Fig. 3). Most probably these particles were created in the gas phase and then deposited onto the substrate as it was discussed before for the cyclopropylamine plasma.[25] Hence, at a higher working pressure

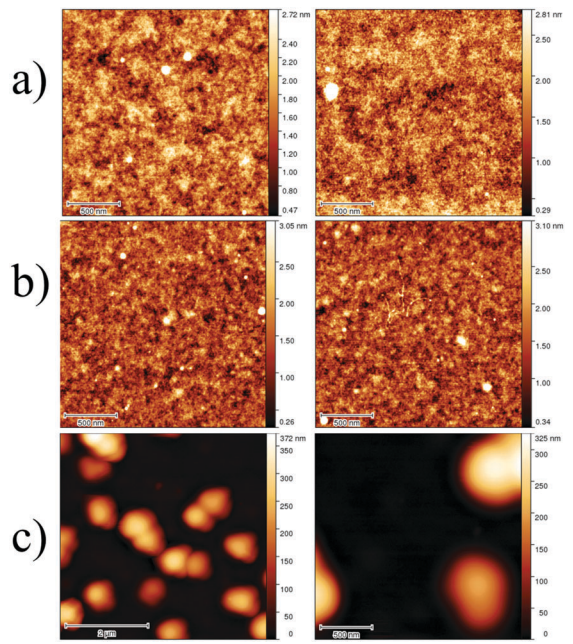

Fig. 3 AFM topographical image of the AGE plasma polymers deposited at W/F = 9.8 eV per molecule and at pressures of 10 (a), 15 (b) and 30 Pa (c) before (on the left) and after (on the right) immersion in water for 24 h.

and consequently at a lower bias, the deposited film is less dense and compact. According to AFM the rms roughness (R_{rms}) of the AGE plasma polymers deposited at 10 and 15 Pa was $\leq$1 nm.

3.1.2 The AGE plasma polymer chemistry. Regarding the chemistry of the AGE plasma polymers, FT-IR analysis (Fig. 4) of the sample deposited at 15 Pa and W/F = 3.9 eV revealed several finger-print peaks of the epoxy group including epoxide ring breathing (1253 cm^{-1}), antisymmetric epoxide ring deformation (913 cm^{-1}), and symmetric epoxide ring deformation (845 cm^{-1}). Additionally, weak C–H stretching of an epoxide was found at 3054 cm^{-1}. In addition to the epoxy group peaks, the FT-IR spectrum displayed symmetric and asymmetric C–H stretching of the aliphatic carbon (most probably C–H_2) at 2873 and 2931 cm^{-1}, respectively. The peaks at 1670 and 1720 can be attributed to C=C and C=O stretching, respectively. Most likely, C=C were grafted into the AGE plasma polymers *via* the opening of the epoxide ring, whereas the carbonyl groups C=O (aldehydes or carboxylic acid) could have been formed by monomer degradation in the plasma. The combined intensity of the epoxide ring breathing and symmetric epoxide ring deformation normalized over the film thickness is plotted as a function of pressure (at W/F = 3.9 eV per molecule) in Fig. 5. The normalized intensities of both peaks increase with pressure suggesting the higher retention of the monomer structure with pressure.

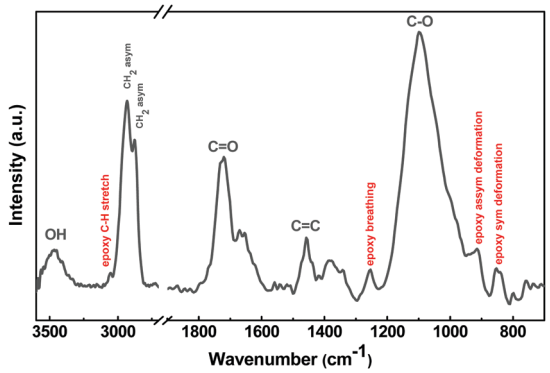

Fig. 4 Typical FT-IR spectrum of the AGE plasma polymer deposited at p = 15 Pa and W/F = 3.9 eV per molecule.

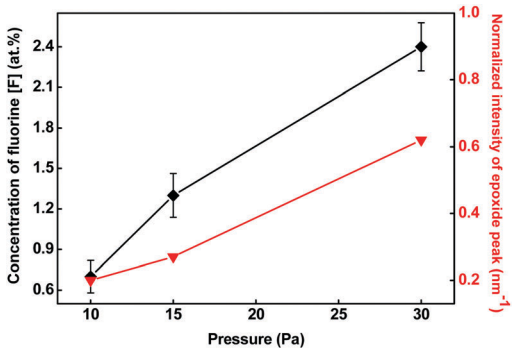

Fig. 5 The normalized combined intensity of epoxide ring deformations and the density of epoxy groups measured through a reaction with TFEA as a function of pressure at fixed W/F = 3.9 eV per molecule.

In order to compliment the FT-IR observations, the AGE plasma polymers were analyzed by XPS. According to the XPS analysis, regardless of pressure and W/F, the AGE plasma polymers are composed exclusively of carbon and oxygen (Table 1).

The carbon environment was analyzed by fitting the C1 spectra. The C1s curve fit was performed according to the methodology reported by Tarduci *et al.* The C1s signal was fitted with a sum of five components, namely hydrocarbons CH_x (BE = 285.0 eV, used for calibration of the BE scale), carbon singly bonded to oxygen C–O (BE = 286.55 eV $\pm$ 0.03 eV), carbon of the epoxide C–O–C (BE = 287 $\pm$ 0.03 eV), carbon doubly bonded to oxygen C=O (BE = 287.8 $\pm$ 0.05 eV) and the ester/carboxyl group COOR (BE = 289 $\pm$ 0.05 eV). The full width at a half maximum for all peaks was set to 1.4 $\pm$ 0.1 eV.

The C1s spectra obtained for AGE plasma polymers deposited at different pressure (and fixed W/F = 3.9 eV per molecule) are reported in Fig. 6. For the reader's convenience, a simulated spectrum of "ideally" polymerized AGE is also plotted in the figure. The BE and FWHM for CH_x, C–O and C–O–C were set to the same values as used in curve fitting of real AGE plasma polymers. The intensity for each carbon environment was set to 33.3% with respect to the AGE chemical formula. Obviously, none of the experimental spectra of AGE plasma polymers matched the "ideal" AGE polymer structure. First of all, whatever the pressure, the COOR and C=O contributions were detected on the surface of the AGE plasma polymer, even though such carbon environments are not present in the AGE structure and cannot be formed by free radical polymerization. Both these contributions most likely arise from monomer fragmentation in the plasma or from the inevitable oxidation upon subsequent contact with air. However, it can be noticed that the intensities of the peaks decrease with pressure. More importantly, the increase of pressure from 10 to 15 Pa led to the appearance of the epoxide contribution C–O–C. The intensity of this component increased by a factor of 2.4 for a pressure of 30 Pa (as compared to 15 Pa). Additionally, the intensity of the CH_x contribution decreased significantly with pressure while the shape of the C1s peak approached more the shape of the "ideal" AGE polymer.

One might have doubts regarding the separation of the epoxide group from other oxidized carbon environments (C–O and C=O)

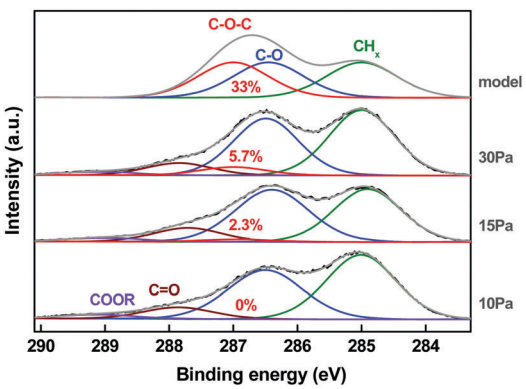

Fig. 6 XPS C1s curve fit for AGE plasma polymers deposited at three different pressures (at fixed W/F = 3.9 eV) as well as the simulated spectrum of an ideal AGE polymer.

due to their proximity on the binding energy scale. Therefore, in order to confirm the reliability of the curve fitting, the AGE plasma polymers were chemically derivatized with TFEA (Fig. 1b). As shown in Fig. 5, the concentration of the chemical marker, *i.e.* fluorine, increases with pressure similarly to the trend observed for the intensity of the epoxide ring vibrations in FTIR and for the C–O–C component in XPS. Hence, all three techniques, aiming at the investigation of the epoxy group density, exposed one by one similar behavior with increasing pressure.

The positive effect of pressure on the degree of epoxide group incorporation can be attributed to two factors. First of all, through the pressure increase, the D.C. self-bias was significantly reduced (Fig. 2) leading to considerably softer ion bombardment of the growing film. Secondly, Saboohi *et al.* showed with the help of *in situ* mass spectrometry of the plasma phase that by increasing the pressure from 2.6 to 8 Pa the fragmentation of the precursor in the gas phase is significantly decreased.[26] Hence "soft landed ions" can help to retain better the monomer structure in the growing film while the functional groups can be more easily deposited from the weakly/less heavily fragmented plasma phase.

3.1.3 The AGE plasma polymer stability in water. Concerning the stability of the AGE plasma polymers in water, it was found that after 24 hour long immersion the layers deposited at 10 and 15 Pa exhibited a negligible thickness loss (less than 1%, ~2 nm), whereas the AGE plasma polymer deposited at 30 Pa lost about 12% of its thickness (~23 nm). Moreover, AFM revealed that the nanoparticles of the AGE plasma polymer deposited at 30 Pa disappeared. In contrast, the morphology of layers deposited at 15 Pa was not affected by immersion in water.

Therefore, despite the very positive effect of the pressure rise on the density of epoxy groups, further optimization of the AGE plasma polymerization was carried out at a fixed pressure of 15 Pa. At this pressure the density of epoxy groups was shown to be increased (as compared to 10 Pa) while the stability of the layer does not need to be compromised (as opposed to 30 Pa).

3.2 Influence of W/F

3.2.1 Influence of W/F on the AGE plasma polymer stability. The stability of the AGE plasma polymers was found to be affected by W/F. For example, the layers deposited at 15 Pa (henceforth, the actual working pressure) exhibited a thickness loss of less than 6% for W/F in the range from 1.9 to 18.6 eV per molecule. The chemical stability of AGE plasma polymers over the range of W/F values is reflected in the change of normalized intensities of epoxide peaks before and after immersion in water (Fig. 7). It should be noted that the values for normalized intensities of epoxide ring deformations after immersion are rather similar to the corresponding initial values before immersion indicating that the AGE plasma polymers deposited at 15 Pa remain relatively stable over a wide range of W/F.

3.2.2 Influence of W/F on the AGE plasma polymer chemistry. Although the concentrations of carbon and oxygen did not change significantly with W/F (see Table 1), the composite parameter affected the chemical structure of the deposited AGE plasma polymers as suggested by the FT-IR findings and the XPS C1s curve fit. The normalized intensities of the two most characteristic

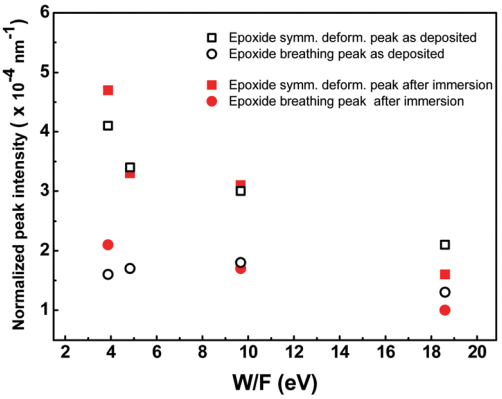

Fig. 7 The normalized intensity of the FTIR peaks for AGE plasma polymers after immersion in water for 24 h as a function of W/F.

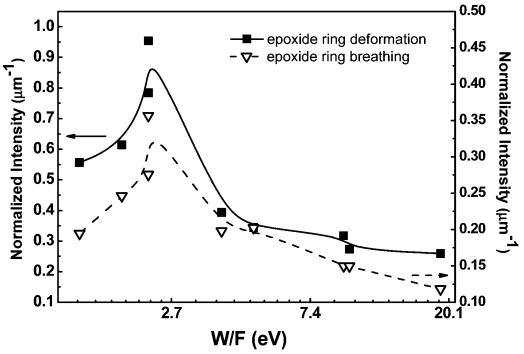

Fig. 8 Normalized intensities of the characteristic FTIR epoxide ring peaks as a function of W/F.

peaks of the epoxide ring (1253 and 845 cm^{-1}) and the concentrations of different carbon environments are presented as a function of W/F in Fig. 8 and 9, respectively. In order to emphasize important changes observed especially in the low W/F range, the data are plotted on a logarithmic scale. Both the normalized IR peak intensities of the epoxide and the C–O–C component exhibit very similar behavior over the entire W/F range reaching a maximum at around 2.3 eV per molecule. In the interval from 2.3 to 18.6 eV per molecule the intensities of epoxide ring peaks and the C–O–C contribution decrease with

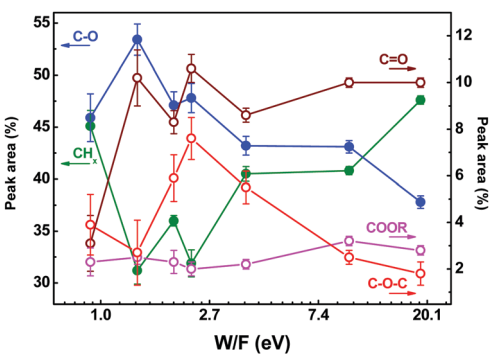

Fig. 9 The dependence of carbon environments (corresponding peak areas derived from the XPS C1s peak fit) as a function of W/F.

an exponential decay, whereas the $\underline{C}H_x$ component increases. Such behavior is generally associated with more extensive fragmentation of the monomer in the plasma due to the increase of the energy invested per monomer molecule with power.[15,25,27–30] However, in the range of rather low W/F (0.91–2.3 eV per molecule) a significant decrease of epoxide ring intensity and $\underline{C}$–O–$\underline{C}$ with decreasing W/F is observed.

4 Discussion

The presence of a maximum on the curves presented in Fig. 8 and 9 suggests that for the AGE precursor the general assumption that higher quality of the plasma polymer (*i.e.* a higher density of the target functional group) can be achieved through a decrease of the power input is, in fact, not relevant. This effect can be attributed to the mechanism of AGE plasma polymerization. Indeed, the rather complex structure of the AGE molecule contains many reactive bonds that can be activated by interaction with plasma species *via* a multitude of reaction pathways. At a high W/F ($\geq$3 eV per molecule) any bond in AGE can be randomly broken in the plasma and the density of the epoxides will be thus limited by this heavy fragmentation. Furthermore, even those epoxide rings which were retained during the T_{OFF} period, are, in their turn, exposed to intensive ion bombardment due to a higher self-bias. However, when the energy input is significantly reduced (below 2.3 eV per molecule), the difference in bond dissociation energies will play a key role in the sequence of bond scissions.

In order to estimate which bonds would be more likely to break at the lowest energy, *ab initio* calculations of the dissociation energy for every bond in the AGE molecule were performed (Fig. 10).

The comparison of the epoxide C–O bond dissociation energy with the dissociation energies of other chemical bonds in the AGE molecule makes it evident that that a difference of ~1 eV can be crucial for epoxide group retention. In other words, when the energy of the excited species is rather low (<3.27 eV), the only activated group will be the epoxide ring and the deposited material will, consequently, contain no epoxide rings at all. Although the electron temperature in the plasma is not influenced by the RF power, the concentration of more energetic electrons will significantly decrease at low W/F, because of the decrease of the electron density at low power. This is partially confirmed by the extremely low deposition rate (0.25 nm min^{-1} at W/F = 0.91 eV per molecule as compared to 1.6 nm min^{-1} at W/F = 2.3 eV per molecule) and the drop in the epoxide peak intensities in FT-IR as well as the $\underline{C}$–O–$\underline{C}$ component in XPS over the range of W/F from 0.91 to 2.3 eV per molecule. The *ab initio* calculations well matched the mass spectrometry data of AGE reported in ref. 31, showing that the highest intensities of the ions are formed due to decomposition of the epoxide ring, but some ions can be also attributed to the decomposition of the ether bond. In addition, the calculations revealed that the C–O scission of ether has a lower energy than the dissociation of C–C bonds, which also matches well the mass spectrometry data of ethyl trimethyl acetate plasma.[32] Hence the scission of ether bonds (and not C=C or C–C bonds) could lead to the formation of radical containing epoxide rings but this process will be very much limited.

Interestingly, the density of epoxide groups on the surface of the AGE plasma polymer is significantly lower in comparison to the GMA plasma polymerization results reported by Tarducci *et al.*[9] The same methodology of *ab initio* calculations was used to estimate the dissociation energy for every bond in the GMA molecule (Fig. 11). Similarly to the AGE *ab initio* calculation results, the weakest bond in the GMA structure belongs as well to the epoxide ring. However, for GMA the energy difference between singlet and triplet states which correspond to double C=C bond conversion to a single C–C bond is lower by 0.54 eV as compared to AGE. This difference can be attributed to the presence of an additional C=O group in the structure of the GMA molecule. The oxygen atom in this carbonyl group attracts electronic density to itself due to its higher value of electronegativity in comparison to carbon atoms and contributes, thus, to the weakening of the nearby C=C bond.

The aforementioned computational results demonstrate that for both AGE and GMA molecules the most reactive group is the epoxide group. Therefore, in order to improve substantially the density of epoxy groups on the surface of a plasma polymer, the choice of the monomer is a crucial parameter. As mentioned in the introduction, GMA was found to be highly toxic and carcinogenic and, therefore, other precursors must be selected.

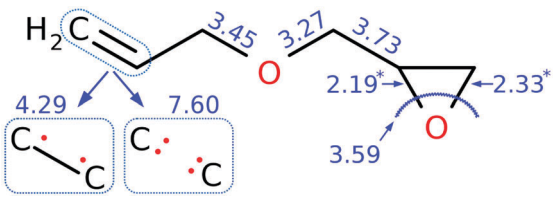

Fig. 10 *Ab intitio* calculation of bond energies in the AGE molecule.

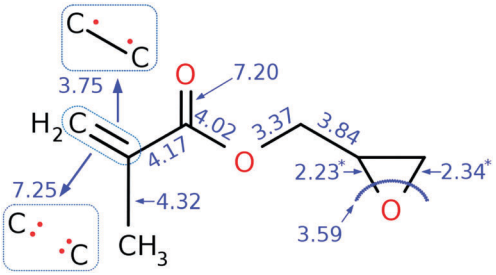

Fig. 11 *Ab initio* calculation of bond energies in the GMA molecule.

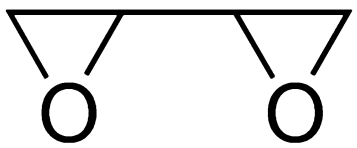

Fig. 12 Chemical structure of 1,3-butadiene diepoxide.

Ab initio calculations point out that the epoxide groups will generally exhibit the lowest bond dissociation energy and will thus have the highest probability of being first fragmented in the plasma. As a consequence, the ideal precursor should be a molecule containing at least two epoxide rings in its structure, *e.g.* 1,3-butadiene diepoxide (Fig. 12).

5 Conclusions

The synthesis of epoxy-rich layers by plasma polymerization is an extremely challenging task. Many experimental parameters might affect the density of epoxide groups on the surface of a plasma polymer. In the current study, it is shown that through the increase of the working pressure it is possible to sufficiently augment the concentration of epoxide groups. However, the layers deposited at a higher pressure exhibit a worse stability in water. According to our results, the optimal working pressure for AGE plasma polymerization is 15 Pa. The composite parameter W/F also plays an important role in affecting the density of epoxides. At 15 Pa the optimal value of 2.3 eV, leading to the highest density of epoxides, was revealed through the FTIR and XPS findings. The *ab initio* calculations suggested that the lowest bond dissociation energy belongs to the C–O bond of the epoxide ring. When the energy input is extremely low (less than 2.3 eV per molecule), epoxides mainly become dissociated in the plasma and as a result very little material, which is almost completely epoxy-free, is deposited. Therefore, in order to improve the density of epoxy groups synthesized through plasma polymerization, it is necessary to change the precursor. The ideal precursor can be a molecule containing at least two epoxide rings, *e.g.* 1,3-butadiene diepoxide.

Conflicts of interest

There are no conflicts to declare.

Acknowledgements

Authors gratefully acknowledge the financial support of the Ministry of Education and Science of the Russian Federation in the framework of Increase Competitiveness Program of NUST "MISiS" (K4-2016-005), implemented by a governmental decree dated 16th of March 2013, N 211. Authors also acknowledge the project CEITEC 2020 (LQ1601) with financial support from the Ministry of Education, Youth and Sports of the Czech Republic (MEYS CR) under the National Sustainability Programme II. Part of the work was carried out with the support of CEITEC Nano Research Infrastructure (MEYS CR, 2016–2019). MM is a Brno PhD Talent scholarship holder – funded by Brno city municipality.

References

1 J. H. Myung, C. a. Launiere, D. T. Eddington and S. Hong, Enhanced tumor cell isolation by a biomimetic combination of e-selectin and anti-epcam: Implications for the effective separation of circulating tumor cells (CTCs), *Langmuir*, 2010, **26**, 8589–8596.

2 J. H. Myung, K. a. Gajjar, J. Chen, R. E. Molokie and S. Hong, Differential detection of tumor cells using a combination of cell rolling, multivalent binding, and multiple antibodies, *Anal. Chem.*, 2014, **86**, 6088–6094.

3 V. Montaño-Machado, L. Hugoni, S. Díaz-Rodríguez, R. Tolouei, P. Chevallier, E. Pauthe and D. Mantovani, A comparison of adsorbed and grafted fibronectin coatings under static and dynamic conditions, *Phys. Chem. Chem. Phys.*, 2016, **18**, 24704–24712.

4 W. Xie, L.-T. Weng, C.-K. Chan, K. L. Yeung and C.-M. Chan, Reactions of SO_2 and NH_3 with epoxy groups on the surface of graphite oxide powder, *Phys. Chem. Chem. Phys.*, 2018, **20**, 6431–6439.

5 M. Khan, S. Schuster and M. Zharnikov, Chemical derivatization and biofunctionalization of hydrogel nanomembranes for potential biomedical and biosensor applications, *Phys. Chem. Chem. Phys.*, 2016, **18**, 12035–12042.

6 L. Shechter, J. Wynstra and R. P. Kurkjy, Glycidyl Ether Reactions with Amines, *Ind. Eng. Chem.*, 1956, **48**, 94–97.

7 C. Funk, P. M. Dietrich, T. Gross, H. Min, W. E. S. Unger and W. Weigel, Epoxy-functionalized surfaces for microarray applications: Surface chemical analysis and fluorescence labeling of surface species, *Surf. Interface Anal.*, 2012, **44**, 890–894.

8 J. A. Howarter and J. P. Youngblood, Optimization of silica silanization by 3-aminopropyltriethoxysilane, *Langmuir*, 2006, **22**, 11142–11147.

9 C. Tarducci, E. J. Kinmond, J. P. S. Badyal, S. A. Brewer and C. Willis, Epoxide-Functionalized Solid Surfaces, *Chem. Mater.*, 2000, **12**, 1884–1889.

10 C. Klages, H. Katrin and N. Kl, Surface Functionalization at Atmospheric Pressure by DBD-Based Pulsed Plasma Polymerization 1, *Plasmas Polym.*, 2000, **5**, 79–89.

11 N. D. Boscher, F. Hilt, D. Duday, G. Frache, T. Fouquet and P. Choquet, Atmospheric pressure plasma initiated chemical vapor deposition using ultra-short square pulse dielectric barrier discharge, *Plasma Processes Polym.*, 2015, **12**, 66–74.

12 G. Camporeale, M. Moreno-Couranjou, S. Bonot, R. Mauchauff, N. D. Boscher, C. Bebrone, C. Van de Weerdt, H. M. Cauchie, P. Favia and P. Choquet, Atmospheric-Pressure Plasma Deposited Epoxy-Rich Thin Films as Platforms for Biomolecule Immobilization-Application for Anti-Biofouling and Xenobiotic-Degrading Surfaces, *Plasma Processes Polym.*, 2015, **12**, 1208–1219.

13 B. Thierry, M. Jasieniak, L. C. P. M. de Smet, K. Vasilev and H. J. Griesser, Reactive epoxy-functionalized thin films by a pulsed plasma polymerization process, *Langmuir*, 2008, **24**, 10187–10195.

14 B. R. Coad, M. Jasieniak, S. S. Griesser and H. J. Griesser, Controlled covalent surface immobilisation of proteins and peptides using plasma methods, *Surf. Coat. Technol.*, 2013, **233**, 169–177.

15 A. Manakhov, L. Zajíčková, M. Eliáš, J. Čechal, J. Polčák, J. Hnilica, Š. Bittnerová and D. Nečas, Optimization of Cyclopropylamine Plasma Polymerization toward Enhanced

Layer Stability in Contact with Water, *Plasma Processes Polym.*, 2014, **11**, 532–544.
16 D. Franta, D. Nečas and L. Zajickova, Models of dielectric response in disordered solids, *Opt. Express*, 2007, **15**, 373–384.
17 D. Nečas, I. Ohlídal and D. Franta, Variable-angle spectroscopic ellipsometry of considerably non-uniform thin films, *J. Opt.*, 2011, **13**, 85705.
18 G. Beamson and D. Briggs, *High resolution XPS of organic polymers*, John Wiley & Sons, Chichester, England, 1992.
19 A. Stoica, A. Manakhov, J. Polčák, P. Ondračka, V. Buršíková, R. Zajíčková, J. Medalová and L. Zajíčková, Cell proliferation on modified DLC thin films prepared by plasma enhanced chemical vapor deposition, *Biointerphases*, 2015, **10**, 029520.
20 A. D. Becke, Density-functional thermochemistry. III. The role of exact exchange, *J. Chem. Phys.*, 1993, **98**, 5648–5652.
21 C. Lee, W. Yang and R. G. Parr, Development of the Colle-Salvetti correlation-energy formula into a functional of the electron density, *Phys. Rev. B: Condens. Matter Mater. Phys.*, 1988, **37**, 785–789.
22 M. W. Schmidt, K. K. Baldridge, J. A. Boatz, S. T. Elbert, M. S. Gordon, J. H. Jensen, S. Koseki, N. Matsunaga, K. A. Nguyen, S. Su, T. L. Windus, M. Dupuis and J. A. Montgomery, General atomic and molecular electronic structure system, *J. Comput. Chem.*, 1993, **14**, 1347–1363.
23 S. Do Lee, B. M. Kim, D. W. Kim, M. Il Kim, K. R. Roshan, M. K. Kim, Y. S. Won and D. W. Park, Synthesis of cyclic carbonate from carbon dioxide and epoxides with polystyrene-supported quaternized ammonium salt catalysts, *Appl. Catal., A*, 2014, **486**, 69–76.
24 J. Tharun, G. Mathai, A. C. Kathalikkattil, R. Roshan, J.-Y. Kwak and D.-W. Park, Microwave-assisted synthesis of cyclic carbonates by a formic acid/KI catalytic system, *Green Chem.*, 2013, **15**, 1673.
25 A. Manakhov, M. Landová, J. Medalová, M. Michlíček, J. Polčák, D. Nečas and L. Zajíčková, Cyclopropylamine plasma polymers for increased cell adhesion and growth, *Plasma Processes Polym.*, 2017, **14**, e1700123.
26 S. Saboohi, B. R. Coad, H. J. Griesser, A. Michelmore and R. D. Short, Synthesis of highly functionalised plasma polymer films from protonated precursor ions *via* the plasma α–γ transition, *Phys. Chem. Chem. Phys.*, 2017, **19**, 5637–5646.
27 D. Hegemann, E. Körner and S. Guimond, Plasma polymerization of acrylic acid revisited, *Plasma Processes Polym.*, 2009, **6**, 246–254.
28 F. Khelifa, S. Ershov, Y. Habibi, R. Snyders and P. Dubois, Free-Radical-Induced Grafting from Plasma Polymer Surfaces, *Chem. Rev.*, 2016, **116**, 3975–4005.
29 S. Ershov, F. Khelifa, V. Lemaur, J. Cornil, D. Cossement, Y. Habibi, P. Dubois and R. Snyders, Free Radical Generation and Concentration in a PlasmaPolymer: The Effect of Aromaticity., *ACS Appl. Mater. Interfaces*, 2014, **6**, 12395–12405.
30 S. Ershov, F. Khelifa, P. Dubois and R. Snyders, Derivatization of free radicals in an isopropanol plasma polymer film: The first step toward polymer grafting, *ACS Appl. Mater. Interfaces*, 2013, **5**, 4216–4223.
31 Y. Yildirim, M. Balcan, A. D. Bass, P. Cloutier and L. Sanche, Electron stimulated desorption of anions and cations from condensed allyl glycidyl ether, *Phys. Chem. Chem. Phys.*, 2010, **12**, 7950–7958.
32 S. Saboohi, H. J. Griesser, B. R. Coad, R. D. Short and A. Michelmore, Promiscuous hydrogen in polymerising plasmas, *Phys. Chem. Chem. Phys.*, 2018, 1–24.